Supplemental Digital Content

Title: Alteration of the fecal microbiome in patients with cholecystectomy: potential relationship with post-cholecystectomy diarrhea - before and after study -

Methods

1. Bacterial DNA extraction and 16S rRNA sequencing from fecal samples

DNA was extracted using a DNeasy PowerSoil Kit (Qiagen, Hilden, Germany) following the manufacturer's instructions. The extracted DNA was quantified using a Quant-IT PicoGreen (Invitrogen). To amplify the V3 and V4 regions of the bacterial genomic DNA, the sequencing libraries were prepared according to Illumina 16S Metagenomic Sequencing Library protocols. The input gDNA 2 ng was polymerase chain reaction (PCR) amplified with 5x reaction buffer, 1 mM deoxynucleotide mix, 500 nM each of the universal forward/reverse PCR primers, and Herculase II fusion DNA polymerase (Agilent Technologies, Santa Clara, CA). The cycle conditions for the 1st PCR was 3 min at 95°C for heat activation, followed by 25 cycles each of 30 s at 95°C, 30 s at 55°C, and 30 s at 72°C, followed by a 5-min final extension at 72°C. The universal primer pair with Illumina adapter overhang sequences used for the first amplification was as follows: V3-F, 5'-TCGTCGGCAGCGTCAGATGTGTATAAGAGACAGCCTACGGGNGGCWGCAG-3' and V4-R 5'-GTCTCGTGGGCTCGGAGATGTGTATAAGAGACAGGACTACHVGGGTATCTAATCC-3'.

The 1st PCR product was purified using AMPure beads (Agencourt Bioscience, Beverly, MA). Following purification, 2 ul of the 1st PCR product was PCR amplified for final library construction containing the index using NexteraXT Indexed Primer. The cycle condition for the 2nd PCR was the same as the 1st PCR condition, except for 10 cycles. The PCR products were purified using AMPure beads. Subsequently, the final purified product was quantified using quantitative PCR (qPCR) according to the qPCR Quantification Protocol Guide (KAPA Library Quantification kits for Illumina Sequencing platforms) and qualified using TapeStation D1000 ScreenTape (Agilent Technologies, Waldbronn, Germany). Paired-end (2 × 301 bp) sequencing was performed by Macrogen using the MiSeq platform (Illumina, San Diego, USA).

2. Data processing for microbial metagenome analysis

Raw data generated by the Illumina MiSeq platform were demultiplexed using index sequences. Adapter sequences and barcode primers were trimmed using Cutadapt (v3.2) program [1]. Preprocessing was performed using the DADA2 (v1.18.0) package in R (v4.0.3) to denoise sequencing errors and identify amplicon sequence variants (ASVs) [2]. Paired-end reads were truncated to 250 bp forward sequences and 200 bp reverse sequences. Reads with expected errors of >2 were discarded. Error-corrected reads were merged into one barcode sequence, and chimeric sequences were filtered

using the consensus method of DADA2. The resulting ASV reads of each sample were downsized to equate the minimum observed sampling depth using quantitative insights into microbial ecology (Quantitative Insights Into Microbial Ecology, QIIME, v1.9) by random selection of reads to compare microbial diversity [3]. Taxonomic classification was performed using the National Center for Biotechnology Information 16S ribosomal RNA DB using BLAST+ (v2.9.0) [4]. Each ASV was defined as the taxon of the best-hit subject from the blast results. When Query coverage was <85%, and the identity of the matched region was <85%, the ASVs were regarded as unassigned. To identify phylogenetic relationships between ASVs, multiple alignments of reads were conducted using the mafft (v7.475) program [5]. Subsequently, a phylogenetic tree was constructed using FastTreeMP (v2.1.10) [6].

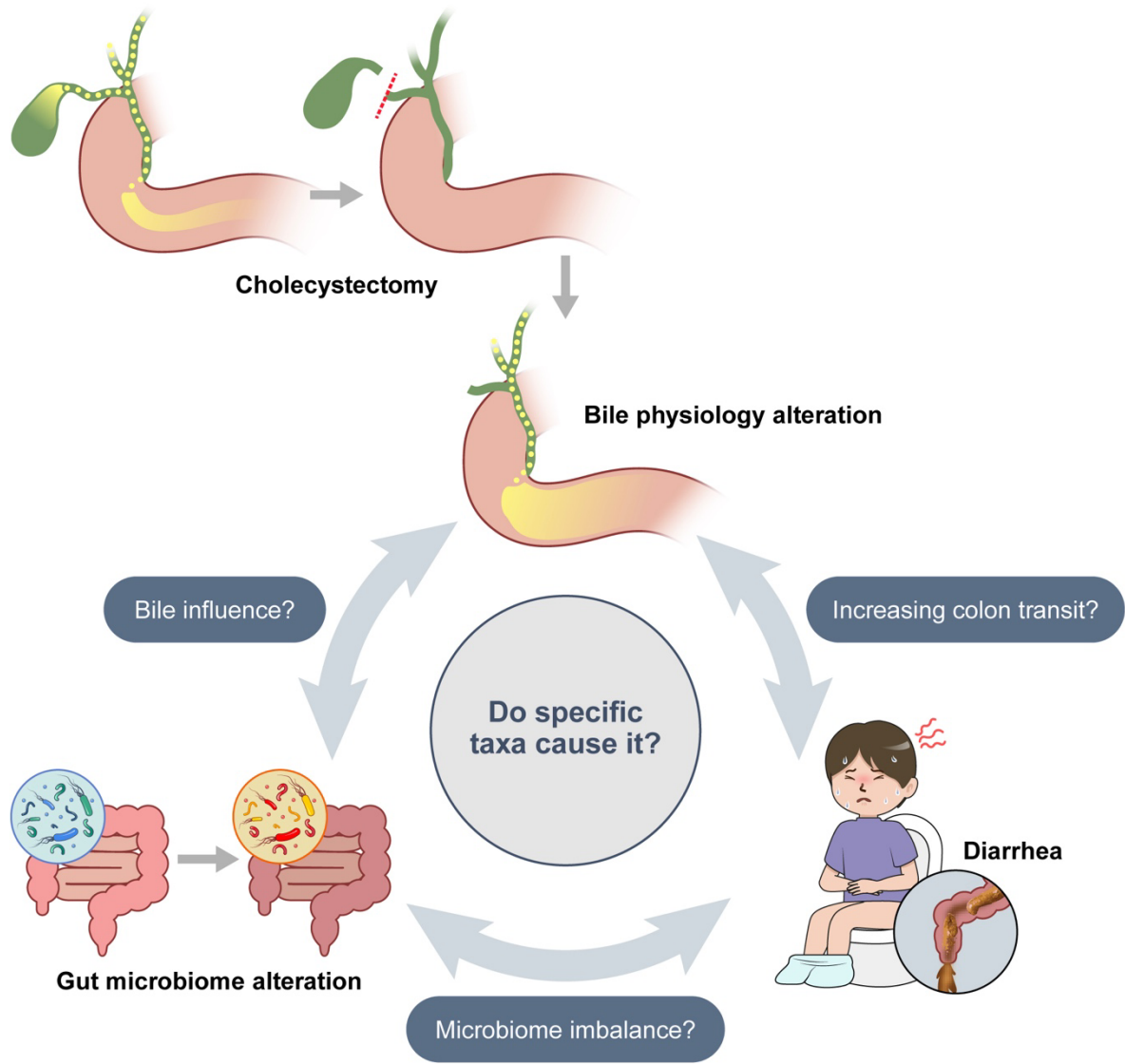## 3. Analysis of bacterial composition and diversity

All taxonomic analyses used relative abundances, defined as ratios, to even sampling depth. Abundances at the phylum, genus, and species levels were averaged to determine the taxonomic composition of each group with a bar graph. The Firmicutes to Bacteroidetes (F/B) ratio was calculated based on their abundance for each patient. The Krona chart, which visualizes complex hierarchies of metagenomic classifications, was constructed using Krona Tools (v2.8.1) [7]. The Krona charts illustrate the average in each group at the species level.

Community diversity was analyzed using QIIME (v1.9.0) [3]. To check the diversity and evenness of the microbial community, the Shannon and Gini–Simpson indices were calculated [8]. In addition, we checked that the rarefaction curves were saturated in all samples to confirm that sequencing depths were sufficient to capture the real diversity [9]. Beta diversities were determined based on weighted and unweighted UniFrac distance metrics, which compared microbial communities by measuring phylogenetic distances [10]. The microbial network was inferred using the SpiecEasi package (v1.1.2) in R (v4.1.2) [11]. The inferred networks were then transformed into an igraph (v1.2.11) object to visualize topological properties [12].

4. Statistical analysis

The Wilcoxon Rank Sum test and Kruskal–Wallis test were conducted to compare the Shannon and Gini–Simpson indices between groups [13, 14]. The false discovery rate of the Benjamini–Hochberg method was performed with a cut-off value of 0.05 to correct errors of multiple testing [15]. The ggpubr R package (v0.4.0) was used to visualize box plots to compare differences in groups for each index [16]. Firmicutes to Bacteroidetes (F/B) ratio is the proportion of two major phyla in the intestinal microflora. An increase or decrease in the F/B ratio indicates an imbalance of the microbiome [17]. The F/B ratio was examined using the Kruskal–Wallis and Dunn tests as a post hoc test with a P-value of 0.05 [18]. In addition, compositional differences among samples were visualized by principal coordinate analysis

(PCoA) [19] and the unweighted pair group method with arithmetic mean tree [20] using unweighted/weighted UniFrac distance metrics. In addition, an analysis of similarities (ANOSIM) statistical test was performed with QIIME script to confirm the significance of differences between groups [3]. Microbes that showed significant differences between groups were identified using the Kruskal–Wallis test and their differences were estimated with a cut-off linear discriminant analysis (LDA) score (log 10) of >2 with linear discriminant analysis effect size (LEfSe) [21]. Furthermore, a cladogram with GraPhlAn (v1.1.3.1) [22] and bar plots were generated using the ggplot R package (v3.3.2). Microbes with a mean abundance of all samples ≥ 1% and significant lists observed from LEfSe were visualized using a heatmap to identify associations between sample groups. Relative abundance data were transformed to log-scale form. Significant taxa from LEfSe were indicated with asterisks. The hierarchical structure calculated using the Euclidean distance was shown as a dendrogram at the top of the plot. Moreover, visualization was performed using ggplot2 (v3.3.5) R package [23]. The accuracy of taxa scoring with high LDA was assessed using the area under the receiver operating curve (AUROC). The pROC R package (v1.18.0) was used to plot the Receiver operating characteristic (ROC) and calculate the AUROC values [24]. Subsequently, the significance of the AUROC was verified using the verification R package [25].

Supplementary Figure 1. Schematic representation of the research hypothesis.

Supplementary Figure 2. Rarefaction curve of all fecal samples.

a1: o_Bacteroidales
a2: c_Bacteroidia
a3: p_Bacteroidetes
a4: f_
a5: g_Phocaeicola
a6: g_Faecalibacterium
a7: s_Faecalibacterium_prausnitzii
a8: p_Proteobacteria
a9: c_Negativicutes
a10: f_Sutterellaceae
a11: o_Burkholderiales
a12: c_Betaproteobacteria
a13: c_Gammaproteobacteria
a14: Bacteria
a15: g_Lachnospira
a16: g_Sutterella
a17: g_Kineothrix
a18: s_Kineothrix_alysoides
a19: s_Lachnospira_eligens
a20: g_Lachnoclostridium
a21: s_Lachnoclostridium_pacaense
a22: s_Sutterella_wadsworthensis
a23: s_Lactobacillus_rogosae
a24: g_Lactobacillus
a25: g_Lacrimispora
a26: s_Lacrimispora_xylanolytica
a27: s_Lachnospira_pectinoschiza
a28: s_Roseburia_inulinivorans
a29: c_Deltaproteobacteria
a30: s_Veillonella_dispar
a31: g_Mitsuokella
a32: g_Enterocloster
a33: s_Mitsuokella_jalaludinii
a34: s_Enterocloster_clostridioformis
a35: s_Oscillibacter_valericigenes
a36: s_Phocaeicola_massiliensis
a37: s_Bacteroides_thetaiotaomicron
a38: o_Desulfovibrionales
a39: f_Desulfovibrionaceae
a40: g_Desulfovibrio
a41: c_Alphaproteobacteria
a42: g_Hungatella
a43: s_Sutterella_stercoricanis
a44: s_Desulfovibrio_intestinalis
a45: s_Negativibacillus_massiliensis
a46: g_Negativibacillus
a47: c_
a48: f_

a49: o_
a50: s_Holdemania_filiformis
a51: g_Pseudoflavonifractor
a52: s_Pseudoflavonifractor_phocaeensis
a53: s_Anaerotignum_faecicola
a54: s_Pseudoflavonifractor_capillosus
a55: g_Holdemania
a56: g_Anaerotruncus
a57: s_[Clostridium]_symbiosum
a58: g_Anaerobium
a59: g_Mobilitalea
a60: s_Mobilitalea_sibirica
a61: s_Anaerobium_acetethylicum
a62: s_Anaerotruncus_rubiinfantis
a63: g_Anaerovorax
b1: p_Firmicutes
b2: c_Clostridia
b3: o_Eubacteriales
b4: g_Ruminococcus
b5: p_Actinobacteria
b6: c_Actinomycetia
b7: g_Bifidobacterium
b8: o_Bifidobacteriales
b9: f_Bifidobacteriaceae
b10: s_Clostridium_saudiense
b11: g_Clostridium
b12: f_Peptostreptococcaceae
b13: f_Eubacteriaceae
b14: s_Ruminococcus_bromii
b15: g_Eubacterium
b16: c_Erysipelotrichia
b17: o_Erysipelotrichales
b18: s_Romboutsia_timonensis
b19: g_Romboutsia
b20: f_
b21: g_Blautia
b22: s_Bacteroides_uniformis
b23: s_Bifidobacterium_faecale
b24: g_Gemmiger
b25: s_Gemmiger_formicilis
b26: c_Coriobacteriia
b27: o_Coriobacteriales
b28: f_Coriobacteriaceae
b29: g_Dorea
b30: g_Collinsella
b31: s_Collinsella_aerofaciens
b32: g_Ligilactobacillus
b33: s_Dorea_longicatena

b34: s_Ligilactobacillus_ruminis
b35: o_Pseudomonadales
b36: g_Monoglobus
b37: s_Monoglobus_pectinilyticus
b38: s_Bifidobacterium_longum
b39: s_Bifidobacterium_catenulatum
b40: p_Verrucomicrobia
b41: s_Akkermansia_muciniphila
b42: g_Akkermansia
b43: c_Verrucomicrobiae
b44: o_Verrucomicrobiales
b45: f_Akkermansiaceae
b46: s_Blautia_luti
b47: s_Catenibacterium_mitsuokai
b48: f_Coprobacillaceae
b49: g_Catenibacterium
b50: f_Moraxellaceae
b51: s_Enterocloster_asparagiformis
b52: f_Streptococcaceae
b53: g_Streptococcus
b54: g_Intestinibacter
b55: s_Intestinibacter_bartlettii
b56: g_Acinetobacter
b57: g_Pseudomonas
b58: f_Pseudomonadaceae
b59: s_Streptococcus_salivarius
b60: s_Staphylococcus_aureus
b61: g_Bacillales
b62: Archaea
b63: s_Micrococcus_aloeverae
b64: s_Blautia_obeum
b65: f_Eggerthellaceae
b66: o_Eggerthellales
b67: c_
b68: f_Staphylococcaceae
b69: g_Staphylococcus
b70: p_Cyanobacteria
b71: o_Oscillatoriales
b72: s_Aerosakkonema_funiforme
b73: g_Aerosakkonema
b74: o_Nostocales
b75: f_Oscillatoriaceae
b76: g_Anaerotignum
b77: g_Klebsiella
b78: s_Acinetobacter_radioresistens
b79: c_Chitinophagia
b80: s_Senegalimassilia_anaerobia
b81: g_Senegalimassilia

b82: s_Acinetobacter_johnsonii
b83: s_Corynebacterium_tuberculostearicum
b84: s_Klebsiella_pneumoniae
b85: o_Corynebacteriales
b86: s_Enterococcus_faecalis
b87: g_
b88: f_Limosilactobacillus
b89: s_[Pseudomonas]_geniculata
b90: f_Chitinophagaceae
b91: f_Xanthomonadaceae
b92: o_Xanthomonadales
b93: f_Enterococcaceae
b94: g_Leptotrichia
b95: g_Enterococcus
b96: s_Ruminiclostridium_sufflavum
b97: s_Tidjanibacter_massiliensis
b98: g_Tidjanibacter
b99: s_Pseudomonas_baetica
b100: g_Moraxella
b101: s_Streptococcus_mitis
b102: s_Weissella_confusa
b103: s_Staphylococcus_caprae
b104: g_Micrococcus
b105: s_Pseudomonas_rhodesiae
b106: o_Sphingomonadales
b107: f_Marinilabiliaceae
b108: g_Latilactobacillus
b109: s_Moraxella_osloensis
b110: g_Weissella
b111: f_Corynebacteriaceae
b112: s_Brevundimonas_naejangsanensis
b113: s_Latilactobacillus_sakei
b114: g_Terrisporobacter
b115: o_Micrococcales
b116: s_Terrisporobacter_petrolearius
b117: s_Clostridium_chauvoei
b118: g_Corynebacterium
b119: g_Victivallis
b120: c_Lentisphaeria
b121: g_Sphingomonas
b122: s_Klebsiella_variicola
b123: f_Sphingomonadaceae
b124: f_Victivallaceae
b125: o_Chitinophagales
b126: s_Limosilactobacillus_reuteri
b127: p_Lentisphaerae
b128: s_Victivallis_vadensis
b129: o_Propionibacteriales

b130: o_Victivallales
b131: o_Marinilabiliales
b132: o_Sphingobacteriales
b133: s_Saccharicrinis_aurantiacus
b134: g_Saccharicrinis
b135: f_Propionibacteriaceae
b136: s_Cutibacterium_acnes
b137: g_Adlercreutzia
b138: g_Cutibacterium
b139: f_
b140: s_Ligilactobacillus_salivarius
b141: f_Bacillaceae
b142: s_Enterococcus_hirae
b143: c_Flavobacteriia
b144: o_Hyphomicrobiales
b145: f_Micrococcaceae
b146: s_Ligilactobacillus_apodemi
b147: s_Pseudomonas_aeruginosa
b148: o_Flavobacteriales
b149: s_Tepidimonas_taiwanensis
b150: o_Cytophagales
b151: c_Cytophagia
b152: f_Sphingobacteriaceae
b153: g_Tepidimonas
b154: g_Methylorubrum
b155: g_Rhizobium
b156: s_Methylorubrum_populi
b157: o_Caulobacterales
b158: f_Lawsonellaceae
b159: g_Lawsonella
b160: g_Bacillus
b161: s_Lawsonella_clevelandensis
b162: s_Ihubacter_massiliensis
b163: f_Caulobacteraceae
b164: g_Ihubacter
b165: c_Sphingobacteriia
b166: g_Neisseria
b167: g_Brevundimonas
b168: f_Neisseriaceae
b169: s_Lactobacillus_johnsonii
b170: f_Rhizobiaceae
b171: o_Neisseriales
b172: s_Adlercreutzia_equolifaciens
b173: f_Weeksellaceae

Supplementary Figure 3. The index of Cladogram (patients with gallstones vs. healthy controls).

Supplementary Figure 4. Comparison of the fecal microbiome in patients with gallstones (GS) after cholecystectomy and healthy controls (HC). (A) Comparison of alpha diversity (Shannon and Gini–Simpson indices) (B) Unweighted UniFrac principal coordinate analysis. GS After cholecystectomy (red dot) vs. HC (green dot). (C) Heat map of taxonomic assignment of fecal samples. The colored columns in the upper part of the heat map indicate GS after cholecystectomy and HC, and those in the lower part of the heat map indicate each participant. Taxonomic abundance is proportional to color intensity (color scale in the upper-left panel of the figure). (D) Krona chart illustrating the differential abundance of bacteria in HC and GS after cholecystectomy. (E) Cladogram highlighting the distribution of the fecal microbiome with differential abundance. (F) Index of the cladogram.
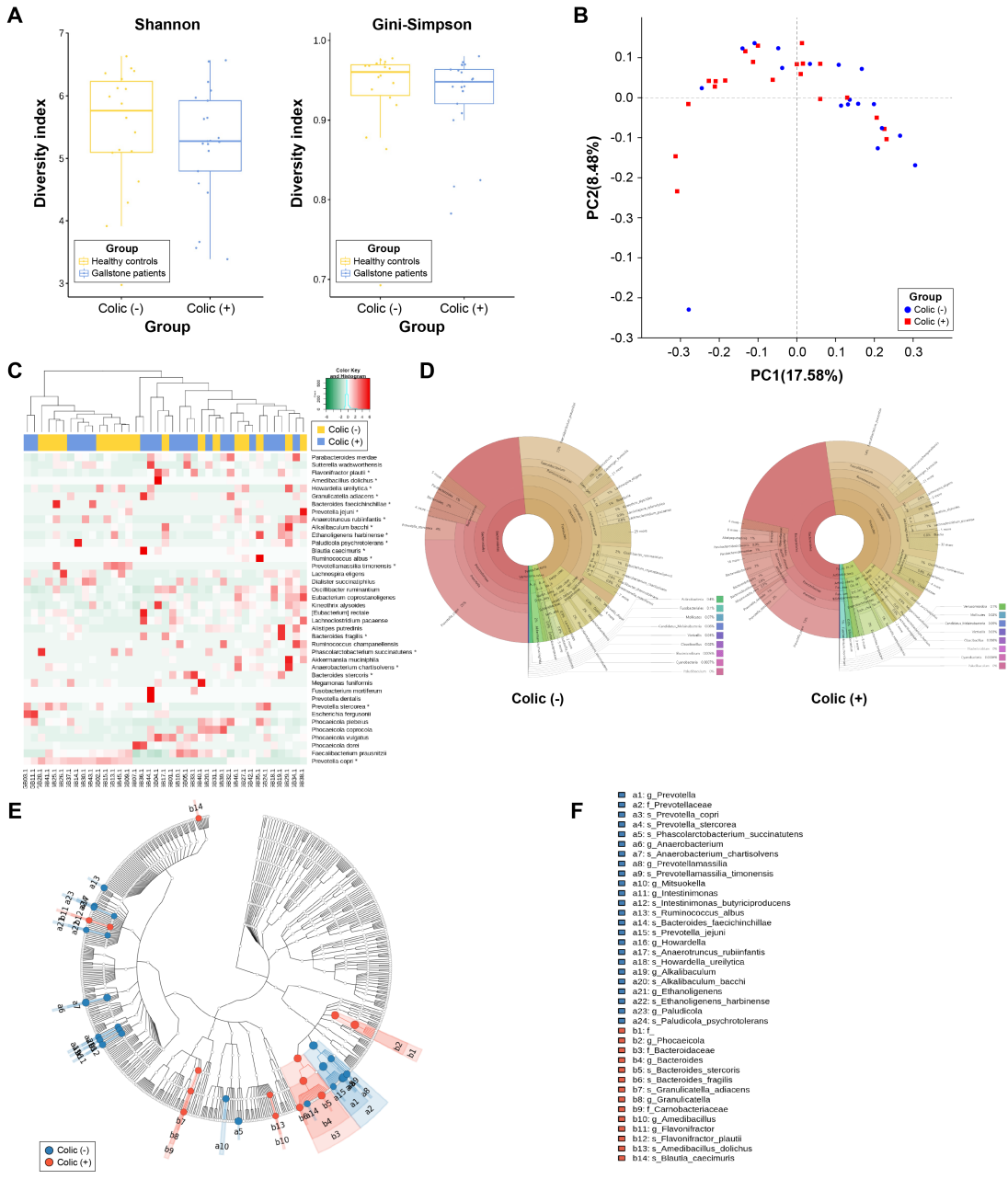
Supplementary Figure 5. Comparison of the gut microbiome in patients with gallstones with typical biliary colic [i.e., colic (+)] and those without symptoms [colic (−)]. (A) Comparison of alpha diversity (Shannon and Gini–Simpson indices) (B) Unweighted UniFrac principal coordinate analysis. Colic (−) (red dot) vs. colic (+) (blue dot). (C) Heat map of taxonomic assignment of fecal samples. The colored columns in the upper part of the heat map indicate patients with colic (−) and colic (+), and those in the lower part of the heat map indicate each participant. Taxonomic abundance is proportional to color intensity (color scale in the upper-left panel of the figure). (D) Krona chart illustrating the differential abundance of bacteria in colic (−) and colic (+). (E) Cladogram highlighting the distribution of the fecal microbiome with differential abundance. (F) Index of the cladogram.

a1: f_Prevotellaceae
a2: s_Prevotella_copri
a3: g_Prevotella
a4: s_Prevotella_stercorea
a5: g_Oscillibacter
a6: f_Eubacteriaceae
a7: g_Eubacterium
a8: s_Oscillibacter_ruminantium
a9: s_Lacrimispora_xylanolytica
a10: g_Lacrimispora
a11: s_Eubacterium_coprostanoligenes
a12: g_Flintibacter
a13: s_Flintibacter_butyricus
a14: s_Intestinimonas_butyriciproducens
a15: g_Intestinimonas
a16: g_Sporobacter
a17: s_Sporobacter_termitidis
a18: g_Duodenibacillus
a19: g_Christensenella
a20: f_Christensenellaceae
a21: s_Duodenibacillus_massiliensis
a22: g_Anaerobacterium
a23: s_Anaerobacterium_chartisolvens
a24: s_Duncaniella_freteri
a25: g_Duncaniella
a26: f_Muribaculaceae
a27: s_[Eubacterium]_siraeum
a28: g_Holdemanella
a29: s_Holdemanella_biformis
a30: s_Coprococcus_eutactus
a31: s_Vallitalea_pronyensis
a32: f_Vallitaleaceae
a33: g_Vallitalea
a34: s_Eubacterium_ruminantium
a35: s_Phocea_massiliensis
a36: g_Phocea
a37: f_Odoribacteraceae
a38: g_Desulfohalotomaculum
a39: s_Anaerotruncus_rubiinfantis
a40: g_Butyricimonas
a41: s_Pseudobutyrivibrio_ruminis
a42: s_Paludicola_psychrotolerans

a43: g_Paludicola
a44: g_Pseudobutyrivibrio
a45: s_Alistipes_finegoldii
a46: g_Anaerotruncus
a47: s_Fournierella_massiliensis
a48: s_Butyricimonas_virosa
a49: g_Fournierella
a50: f_Victivallaceae
a51: s_Anaerotaenia_torta
a52: o_Victivallales
a53: s_Victivallis_vadensis
a54: p_Lentisphaerae
a55: g_Anaerotaenia
a56: g_Victivallis
a57: c_Lentisphaeria
a58: f_Clostridiales_Family_XIII._Incertae_Sedis
a59: g_Ethanoligenens
a60: s_Ethanoligenens_harbinense
b1: f_
b2: g_Phocaeicola
b3: s_Phocaeicola_vulgatus
b4: f_Sutterellaceae
b5: o_Burkholderiales
b6: c_Betaproteobacteria
b7: g_Sutterella
b8: g_Blautia
b9: s_Blautia_wexlerae
b10: s_Dialister_invisus
b11: p_Actinobacteria
b12: o_Bifidobacteriales
b13: f_Bifidobacteriaceae
b14: g_Bifidobacterium
b15: c_Actinomycetia
b16: s_Sutterella_stercoricanis
b17: s_Hungatella_effluvii
b18: s_Bifidobacterium_longum
b19: g_Tyzzerella
b20: g_Collinsella
b21: s_Collinsella_aerofaciens
b22: o_Coriobacteriales
b23: f_Coriobacteriaceae

Supplementary Figure 6. The index of Cladogram in PCD (−) vs. PCD (+) patients. Abbreviation: PCD, post-cholecystectomy diarrhea.

References

1.   Martin M. Cutadapt removes adapter sequences from high-throughput sequencing reads. EMBnet J. 2011;17(1):10-12.

2.   Callahan BJ, McMurdie PJ, Rosen MJ, Han AW, Johnson AJ, Holmes SP. DADA2: high-resolution sample inference from Illumina amplicon data. Nat Methods. 2016;13(7):581-583.

3.   Caporaso JG, Kuczynski J, Stombaugh J, et al. QIIME allows analysis of high-throughput community sequencing data. Nat Methods. 2010;7(5):335-336.

4.   Popovici V, Goldstein DR, Antonov J, Jaggi R, Delorenzi M, Wirapati P. Selecting control genes for RT-QPCR using public microarray data. BMC Bioinformatics. 2009;10:42.

5.   Katoh K, Standley DM. MAFFT multiple sequence alignment software version 7: improvements in performance and usability. Mol Biol Evol. 2013;30(4):772-780.

6.   Price MN, Dehal PS, Arkin AP. FastTree 2–approximately maximum-likelihood trees for large alignments. PLoS One. 2010;5(3):e9490.

7.   Ondov BD, Bergman NH, Phillippy AM. Interactive metagenomic visualization in a Web browser. BMC Bioinformatics. 2011;12:385.

8.   Shannon CE, Weaver W. The mathematical theory of communication. Urbana, IL: The University of Illinois Press; 1964. Available at: https://pure.mpg.de/rest/items/item_2383164/component/file_2383163/content. Accessed May 18, 2022.

9.   Gotelli NJ, Colwell RK. Quantifying biodiversity: procedures and pitfalls in the measurement and comparison of species richness. Ecol Lett. 2001;4(4):379-391.

10.   Lozupone C, Knight R. UniFrac: a new phylogenetic method for comparing microbial communities. Appl Environ Microbiol. 2005;71(12):8228-8235.

11.   Kurtz ZD, Muller CL, Miraldi ER, Littman DR, Blaser MJ, Bonneau RA. Sparse and compositionally robust inference of microbial ecological networks. PLoS Comput Biol. 2015;11(5):e1004226.

12.   Csardi G, Nepusz T. The igraph software package for complex network research. InterJournal. 2006; Complex Systems: 1695. https://www.researchgate.net/profile/Gabor-Csardi/publication/221995787_The_Igraph_Software_Package_for_Complex_Network_Rese arch/links/0c96051d301a30f265000000/The-Igraph-Software-Package-for-Complex-Network-Research.pdf. Accessed May 18, 2022.

13.   Bauer DF. Constructing confidence sets using rank statistics. J Am Stat Assoc. 1972;67(339):687-690.

14.   Hollander M, Wolfe DA, Chicken E. Nonparametric statistical methods. 3rd ed. John Wiley & Sons; 2013.

15.   Benjamini Y, Hochberg Y. Controlling the false discovery rate: a practical and powerful

approach to multiple testing. J R Stat Soc Series B Methodol. 1995;57(1):289-300.

16. Kassambara A, Kassambara MA. ggpubr: 'ggplot2' Based publication ready plots. The Comprehensive R Archive Network. Available at: https://cran.r-project.org/web/packages/ggpubr/index.html. Accessed May 18, 2022.

17. Ojima M, Motooka D, Shimizu K, et al. Metagenomic analysis reveals dynamic changes of whole gut microbiota in the acute phase of intensive care unit patients. Digestive diseases and sciences. 2016; 61:1628-1634.

18. Dunn OJ. Multiple comparisons using rank sums. Technometrics. 1964;6(3):241-252.

19. Gower JC. Some distance properties of latent root and vector methods used in multivariate analysis. Biometrika. 1966;53(3-4):325-338.

20. Sokal RR. A statistical method for evaluating systematic relationships. Univ Kansas Sci Bull. 1958;38:1409-1438.

21. Segata N, Izard J, Waldron L, et al. Metagenomic biomarker discovery and explanation. Genome Biol. 2011;12(6):R60.

22. Asnicar F, Weingart G, Tickle TL, Huttenhower C, Segata N. Compact graphical representation of phylogenetic data and metadata with GraPhlAn. PeerJ. 2015;3:e1029.

23. Wickham H. Data analysis. In: ggplot2: elegant graphics for data analysis. 2nd ed. Springer; 2016:189-201.

24. Robin X, Turck N, Hainard A, et al. pROC: an open-source package for R and S+ to analyze and compare ROC curves. BMC Bioinformatics. 2011;12:77.

25. NCAR - Research Applications Laboratory. verification: Weather forecast verification utilities. The Comprehensive R Archive Network. Available at: https://cran.r-project.org/web/packages/verification. Accessed May 18, 2022.